IJE TRANSACTIONS B: Applications Vol. 34, No. 08, (August 2021) 1845-1855

International Journal of Engineering
Journal Homepage: www.ije.ir

Investigating Behavior of Very Large Crude Oil Carrier Ship's Diesel Engine on Handling Stormy Waters

A. Gholami[a], S. A. Jazayeri*[b], Q. Esmaili[c]

[a] *Department of Mechanical Engineering, Ayatollah Amoli Branch, Islamic Azad University, Amol, Iran*
[b] *Department of Mechanical Engineering, K. N. Toosi University of Technology, Tehran, Iran*
[c] *School of Engineering Technology, University of Special Modern Technologies, Amol, Iran*

PAPER INFO

Paper history:
Received 07 April 2021
Received in revised form 21 May 2021
Accepted 21 June 2021

Keywords:
Diesel Engine
Very Large Crude Oil Carrier
Fuel Consumption
Emissions
Sea Wave and Wind
Mean Value Engine Model

ABSTRACT

The behavior of ship engine encountering stormy waters with different sea wavelengths has been investigated. In this study, a mathematical model is developed using governing equations for various parts of the ship, that is the hull, engine, power transmission shafts from the engine to the propeller also the propeller of the ship itself were implemented in MATLAB/ Simulink software environment. The model consists of the torsional vibrations of the transmission shafts; this enables a more accurate analysis of the engine behavior which is the source of power generation in the ship's propulsion system. The simulation results showed that the wavelength of sea waves has a significant effect on the dynamic performance of the engine. In this research, the effect of different ratios of wavelength to ship length (λ/L_{PP}) including 0.5, 1, 1.5 and 2 in violent stormy sea conditions with a wave height of 11.5 m and wind speed of 28.5 m/s has been investigated. The results showed that with the exception of λ/L_{PP} of 1.5, at another ratios of λ/L_{PP}, changes in engine performance parameters such as torque, fuel and air consumption, CO_2 emission and power are decreasing with increasing wavelength. Most variations in engine speed are related to λ/L_{PP} of 2. The results showed that by reducing the wavelength, the period of oscillations is reduced. As the ratio of wavelength to ship length increases, the number of oscillating points in the engine behavior increases and the lowest number of oscillating points can be seen at λ/L_{PP} of 1.5. This study highlights the importance of effects of sea wavelengths as one of the most important physical parameters of the sea which should not be ignored in the design phase of the ship propulsion system and engine selection.

***doi**: 10.5829/ije.2021.34.08b.05*

1.INTRODUCTION

Today, ship efficiency, energy consumption and strict environmental regulations taking a major impact on marine company's performance [1-3]. Ship propulsion systems are commonly designed to be effective in calm waters. Usually 15-30% of the power required in calm waters is considered as the sea margin to provide the extra power needed in the face of adverse weather conditions [4]. However, due to the uncertain behavior of the waves [5-9] and its effect on the performance of the ship, it is difficult to choose a sea margin, which is reliable and provides the minimum power required in all adverse weather conditions. Waves does affect the size selection of the main engine which adds resistance on the ship or changing the operating point of the main engine, which affects both fuel consumption and emissions. It is common practice that the ship's engine loses some of its torque when

* Corresponding Author Institutional Email: jazayeri@kntu.ac.ir (S. A. Jazayeri)

Please cite this article as: A. Gholami, S. A. Jazayeri, Q. Esmaili, Investigating Behavior of Very Large Crude Oil Carrier Ship's Diesel Engine on Handling Stormy Waters, International Journal of Engineering, Transactions B: Applications, Vol. 34, No. 08, (2021) 1845-1855

dealing with waves, so it is vital important to study the behavior of the engine such as torque, power and fuel consumption in the face of sea waves at earlier stages of ship design or engine selection. Taskar et al. [10, 11] investigated the propeller's emergence and submergence in the face of waves and its effects on the load applied to the engine. Their studies indicated an increase in engine fuel consumption and power in unsteady flows.

Kyrtatos et al. [12] studied the dynamics of the ship and the propeller to optimize the machinery control strategy of the ship's propulsion system. Full scale experiments carried out by Kayano et al. [13] showed that the amount of power delivered by the engine in the face of waves and wind was greater than the amount previously considered at the design stage.

It is very important to have a detail knowledge of the engine performance, as the prime part of the ship's propulsion system. Among the various models such as transfer function models [14], zero or one-dimensional models [15], and multi-zone phenomenological models [16] and cycle Mean Value Engine Models (MVEMs) [12, 17-19] capable of evaluating the engine performance, the mean value engine model (MVEM) has least complexity, much less input data requirements and an adequate calculation execution time. In a transfer function model, which usually represents the relationship of fuel consumption to engine speed, the essential characteristics of the system does not reflect. On the other hand, more accurate results can be achieved using multidimensional models, but achieving these results will be much more time consuming and computationally costly. The basic assumption in the MVEM modeling method is that the air and fuel flows to the cylinder are continuous, so the periodic trend of the engine is ignored and therefore this model can be used to calculate the average time value of engine parameters with a very reasonable accuracy, while the in-cycle variation (e.g. per degree of crank angle) cannot be determined.

In this study, the performance behavior of a very large crude oil carrier (VLCC) ship in the face of sea regular waves of different wavelengths has been investigated using mean value engine model (MVEM). The ship propulsion system model is modularly designed and implemented in Simulink software. As shown in Figure 1, the various components of the ship are defined and implemented as specific blocks in the software environment. Finally, in this research, engine performance parameters such as torque, power, fuel consumption and emissions at different wavelengths have been calculated and examined.

The difference between this paper and other researches is that unlike previous studies in which power transmission shafts were considered only as a rigid body, in the relevant calculations only the mass moment of inertia was considered, but in the present study the power transmission shafts from the engine to the propeller are considered as distributed systems in which the geometric and mechanical properties of

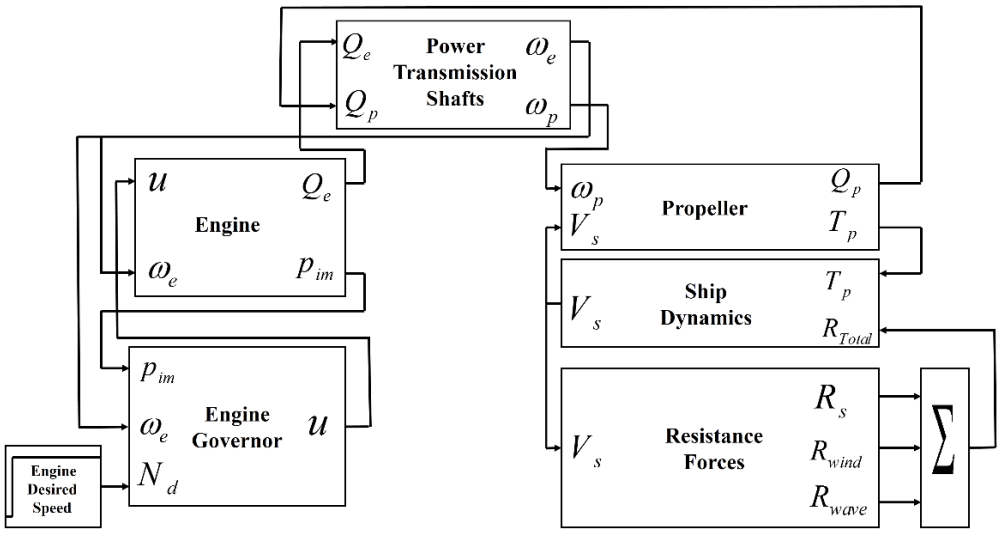

Figure 1. Schematic ship model in Simulink

the shaft such as length, diameter, shear modulus and moment of inertia are applied and coupled to the general model of the ship system. Given the importance of the power-train system in ships, especially in adverse weather conditions, providing a more accurate model of this system will more accurately predict the behavior of the system, especially the ship propulsion engine, in the design or optimization stage.

2. SHIP MODEL

As mentioned earlier, the modular method has been used to model the ship system. Each part of the ship system is a separate block that are interconnected to each other via interfaces. The solver selected in the Simulink environment is ODE45 because it has a high ability to solve ordinary differential equations. The implemented model can be used for low-speed and medium-speed ships, including oil carriers, container ships, bulk carriers and etc.; so the performance parameters of the ship such as speed, power, forces on the ship, fuel consumption, emissions and etc. are calculated.

2. 1. Engine Model The mean value engine model is used to model the engine behavior. In this method, the inflow of air and fuel into the cylinders are assumed continuous and the scavenging and exhaust receivers are assumed thermodynamically open systems [20]. This model includes scavenging and exhaust receivers, cylinders, turbochargers, air cooler, exhaust pipe and engine controller. The governing equations for calculating engine performance are as follows [20, 21]:

$$Q_e = \frac{p_b V_D}{2\pi rev_{cy}}; P_b = \frac{\pi Q_e N_e}{30}; p_b = \frac{60 P_b}{z_{cyl} V_D N_e} \quad (1)$$

where P_b is the engine brake power (watts), p_b is the engine brake mean effective pressure (BMEP), N_e is the engine crankshaft rotational speed (rpm), Q_e is the engine torque, rev_{cy} is revolutions per cycle (2 is for four-stroke engine) and V_D is the engine volume displacement.

The mass flow rate (kg/s) of fuel injected is calculated as follows:

$$\dot{m}_f = \frac{z_{cyl}\, m_{fcycle}\, N_e}{\left(60\ rev_{cy}\right)} \quad (2)$$

where z_{cyl} is the number of engine cylinders, m_{fcycle} is the mass of the fuel injected per cylinder per cycle.

A proportional-integral (PI) controller is used to model the engine governor:

$$u = u_0 + k_p \Delta N + k_i \int \Delta N dt \quad (3)$$

where $\Delta N = N_d - N_e$, N_d is the engine desired speed and N_e is the actual speed, k_i and k_p are the integral and proportional constant, and u_0 is the initial rack position.

The fuel assumed in this model is heavy fuel oil (HFO). The amount of emissions due to combustion can be calculated from the following equation in which *EF* is the emission factor and can be seen in Table 1 for different emissions [22]:

$$m_{ftotal} = \dot{m}_f \Delta t; \dot{m}_i = \dot{m}_f EF_i \quad (4)$$

where Δt is the time interval, m and $\dot{m}$ are mass and mass flowrate, respectively.

To calculate the amount of air passing through the cylinders, considering that the engine is considered to be a two-stroke type, the following equation has been used [20]:

$$\dot{m}_a = C_V A_{Veq} \frac{p_{SC}}{\sqrt{R_{air} T_{SC}}} \sqrt{\frac{2\gamma_A}{\gamma_A - 1}\left(pr_{cyl}^{\frac{2}{\gamma_A}} - pr_{cyl}^{\frac{\gamma_A+1}{\gamma_A}} \right)}; \quad pr_{cyl} = \frac{p_{ER}}{p_{SC}} \quad (5)$$

where C_V is air flow resistance coefficient, A_{Veq} is equivalent effective area, p_{SC} and p_{ER} are scavenging and exhaust receiver's pressures, respectively, pr_{cyl} is cylinder pressure ratio and γ_A is air specific heat ratio. To model the turbocharger behavior, curve fitting and interpolation methods on compressor and turbine performance maps have been used. In the compressor, the volume flow rate of air is a function of the compressor pressure ratio and the rotational speed of the turbocharger, and in the turbine, the gas volume flow rate is a function of the turbine pressure ratio.

The temperature of air exiting the air cooler are calculated as follows:

$$T_{AC} = T_c - \varepsilon(T_c - T_w) \quad (6)$$

TABLE 1. Emission factors [23]

CO_2 (g/g fuel)	NO_X (g/g fuel)	PM (g/g fuel)	SO_X (g/g fuel)
3.114	0.07846	0.00728	0.053

where T_c is the temperature of air exiting the compressor, T_w is the cooling water temperature, and ε is the air cooler effectiveness.

2. 2. Propeller Model The ship propeller is fixed pitch and the relationships of Wageningen propeller type B are used to calculate the dimensionless coefficients of thrust (T_p) and torque (Q_p) [23];

$$T_p = K_T \rho_w N_p^2 D_p^4 \beta; \quad Q_p = K_Q \rho_w N_p^2 D_p^5 \beta^{0.8} \tag{7}$$

where K_T and K_Q are the dimensionless coefficients of thrust and torque, respectively, ρ_w is sea water density, N_p(rev/s) and D_p are the propeller rotational speed and the propeller diameter, respectively and β is thrust diminution factor.

The propeller average wake inflow velocity is affected by ship surge and pitch motions and the waves, based on the available data as follows [24, 25]:

$$V_{Total} = \begin{pmatrix} (1-w_p) \\ \left\{V_S - \omega_e \xi_a \sin(\omega_e t - \zeta_\xi)\right\} \\ +\alpha\omega h_a \exp(-kz_p) \\ \cos X \cos(\omega_e t - k x_p \cos X) \end{pmatrix} \sqrt{\left(1 - \frac{\Delta\bar{p}}{0.5\rho_w V_S^2}\right)} \tag{8}$$

where w_p is effective wake fraction, V_S is ship speed, ω_e is wave encounter circular frequency, ξ_a is surge amplitude, ζ_ξ is phase delay, ω is wave circular frequency, h_a is wave amplitude, k is wave number, z_p is the immersion depth of the propeller shaft, x is the longitudinal distance of the propeller from the center of gravity of the ship, x_p is the position of the propeller section with reference to the center of gravity of the vessel, $\Delta\bar{p}$ is pressure gradient below the bottom of the ship due to pitching motion, X is wave encounter angle (0 for following sea; 180 for head sea), ρ_w is density of seawater, t is time, η_5 is pitch amplitude.

2. 3. Power Transmission Shafts It is assumed that the ship's power transmission shafts from the engine to the propeller are distributed elements. The flywheel and the propeller of the ship are considered lumped elements. The schematic layout of the ship powertrain system is shown in Figure 2. The governing equations of the transmission shafts are as follows [26]:

$$\begin{bmatrix} \omega_1(z_1^{-1}) \\ \omega_2(z_1^{-1}) \end{bmatrix} = 1/\xi_1 \times \begin{bmatrix} \frac{1+z_1^{-1}}{1-z_1^{-1}} & -2\frac{z_1^{-\frac{1}{2}}}{1-z_1^{-1}} \\ 2\frac{z_1^{-\frac{1}{2}}}{1-z_1^{-1}} & -\frac{1+z_1^{-1}}{1-z_1^{-1}} \end{bmatrix} \begin{bmatrix} T_1(z_1^{-1}) \\ T_2(z_1^{-1}) \end{bmatrix}; \tag{9}$$

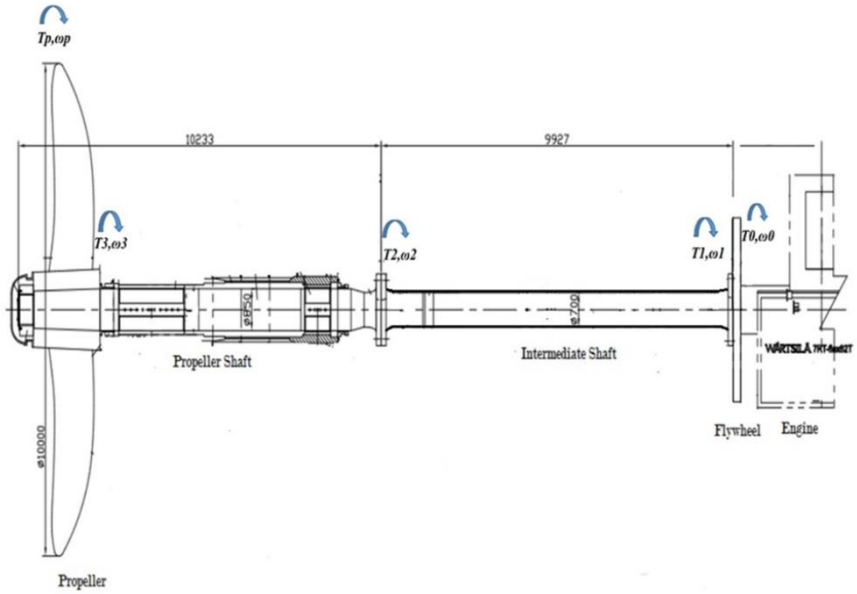

Figure 2. Schematic layout of powertrain system [31]

$$\begin{bmatrix} T_2\left(z_2^{-1}\right) \\ T_3\left(z_2^{-1}\right) \end{bmatrix} = \xi_2 \begin{bmatrix} \frac{1+z_2^{-1}}{1-z_2^{-1}} & -2\frac{z_2^{-\frac{1}{2}}}{1-z_2^{-1}} \\ 2\frac{z_2^{-\frac{1}{2}}}{1-z_2^{-1}} & -\frac{1+z_2^{-1}}{1-z_2^{-1}} \end{bmatrix} \begin{bmatrix} \omega_2\left(z_2^{-1}\right) \\ \omega_3\left(z_2^{-1}\right) \end{bmatrix};$$

$$z_1^{-1} = e^{\left(-2l_1\sqrt{L_1C_1}\right)s}; z_2^{-1} = e^{\left(-2l_2\sqrt{L_2C_2}\right)s}; \xi_1 = \sqrt{\frac{L_1}{C_1}}; \xi_2 = \sqrt{\frac{L_2}{C_2}};$$

$$C_j = \frac{1}{G_j J_{sj}}; L_j = J_{sj}\rho_j \qquad j = 1,2 \tag{10}$$

The governing equations of the flywheel and propeller as lumped elements are as follows:

$$\frac{\omega_f}{T_f}\left(z_1\right) = \frac{\beta_f z_1}{z_1 + \alpha_f}; \beta_f = \frac{1-\alpha_f}{B_f};$$
$$\alpha_f = \exp\left(-\frac{B_f}{J_f} 2l_1\sqrt{\rho_1 / G_1}\right)$$
$$\frac{\omega_p}{T_p}\left(z_2\right) = \frac{\beta_p z_2}{z_2 + \alpha_p}; \beta_p = \frac{1-\alpha_p}{B_p}; \tag{11}$$
$$\alpha_p = \exp\left(-\frac{B_p}{J_p} 2l_2\sqrt{\rho_2 / G_2}\right)$$

where ω_f and ω_p are flywheel and propeller angular speeds, respectively; T_f and T_p are flywheel and propeller torques, respectively. In this case there is not any intermediary parts between intermediate shaft and flywheel; therefore $\omega_e=\omega_0=\omega_1=\omega_f$, where ω_e is engine angular speed. on the other hand, since there is not any intermediary parts between propeller shaft and propeller, therefore $\omega_3=\omega_p$.

2. 4. Ship Dynamic In this research, for modeling the ship motion, only movement in the longitudinal direction is considered. Hence, the governing equation is as follows:

$$\frac{dV_s}{dt} = \frac{(1-t\_d)T_p - (R_S + R_{Add})}{m_{ship} + m_{add}} \tag{12}$$

where V_s is the ship's longitudinal velocity, T_p is the effective propeller thrust, R_S is the ship's resistance which is calculated by the Holtrop method for calm water conditions [27], t_d is the thrust deduction factor, m_{ship} is the ship's mass, m_{add} is the added virtual mass to consider the hydrodynamic force owing to the acceleration of a body in a fluid. The total added resistance (R_{Add}) due to the weather conditions (wave and wind) is estimated using the proposed formula by Liu et al. [28];

$$R_{Add} = R_{AW} + R_{AA} \tag{13}$$

R_{AW} and R_{AA} are added resistance components due to wave and wind, respectively.

3. VALIDATION

The whole ship system was implemented in Simulink environment based on the formulations expressed above. For the model validation, a 12-day VLCC ship fuel consumption measurements report [29] has been used. As shown in Figure 3, there is a good agreement between the simulation results and the

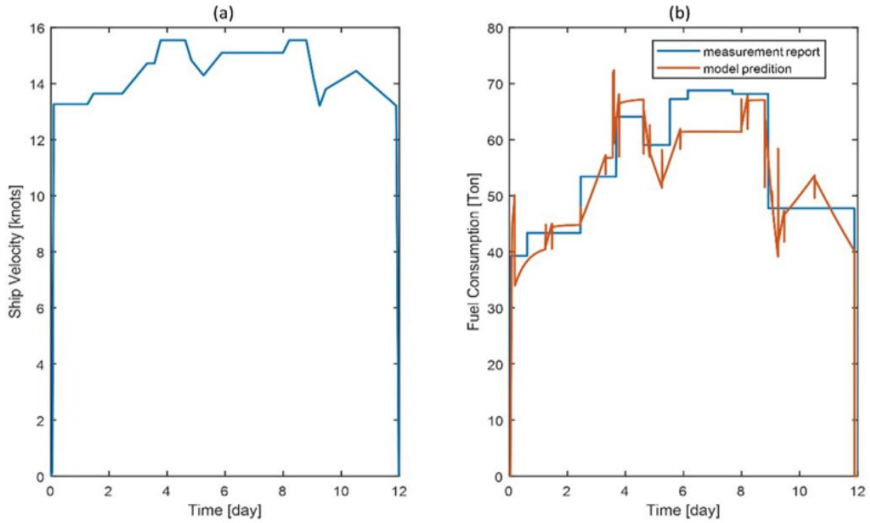

Figure 3. (a) VLCC voyage cycle;(b) fuel consumption

measured report. The maximum difference between the value predicted by the model and the measurement value was 10.82 tons, which is equivalent to 16.1% of the error. The daily average fuel consumption predicted by the model is 49.91 tons and, on the other hand, the measured value is 51.65 tons, which indicates a very good accuracy within 3.5% error.

4. RESULTS AND DISCUSSION

In this section, it is assumed that the ship is facing rough weather conditions. The sea is considered as violent storm with a wave height of 11.5 m and a wind speed of 28.5 m/s according to the ITTC 2017.

The wavelength to the length of ship between perpendicular ratio (λ/L_{PP}) will be 0.5, 1, 1.5 and 2. The ship is in full load condition. It is assumed that the engine desired speed at time 2 s changes from 45 rpm to 80 rpm, which is considered as an input step signal to the model implemented in Simulink. The simulation time is 150 seconds. Using the data in Table 2, simulations were performed at different sea wavelengths. The simulation results including speed, torque, fuel consumption, emitted CO_2 and power are calculated and presented in Figures 4 to 8.

At λ/L_{PP} of 0.5, as shown in Figure 4, the range of engine speed fluctuations at steady-state is between 74.5 and 77.5 rpm. The number of oscillation points is 6. Engine torque fluctuations range is from 2.2 to 3.6 MNm with 9 oscillation points. Fuel consumption

TABLE 2. Ship specifications [30]

Engine		**Intermediate shaft**	
7RT-flex82T	2-stroke	Diameter(d_1)	0.7 [m]
Cylinders no.	7 In-line	Length(l_1)	9.927 [m]
Output (CMCR)	31640 [Kw]	Inertia	1376 [kgm^2]
Propeller		Ultimate-tensile strength (UTS)	590 [N/mm^2]
Blades no.	4	Shear modulus(G_1)	81.4 [GPa]
Diameter (d_p)	9.86 [m]	Density(ρ_1)	7850 [kg/m^3]
Damping (B_p)	467580 [Nms/rad]	**Propeller shaft**	
Load inertia (J_p)	429250 [kgm^2]	Diameter(d_2)	0.85 [m]
Flywheel		Length(l_2)	10.233 [m]
Inertia (J_f)	13600 [kgm^2]	Inertia	3454 [kgm^2]
Damping (B_f)	9115 [Nms/rad]	Ultimate tensile strength(UTS)	590 [N/mm^2]
Ship		Shear modulus(G_2)	81.4 [GPa]
Length (L)	320 [m]	Density (ρ_2)	7850 [kg/m^3]
Breadth (B)	58 [m]		
Displacement volume (V)	312600 [m^3]		
Area of maximum transverse section exposed to the wind (A_{XV})	1161 [m^2]		

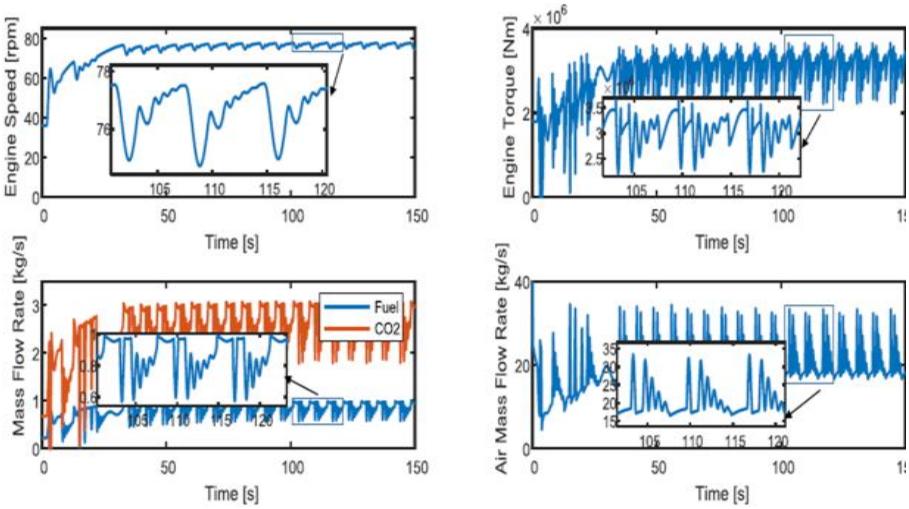

Figure 4. Predicted system response at λ/L_{PP}=0.5

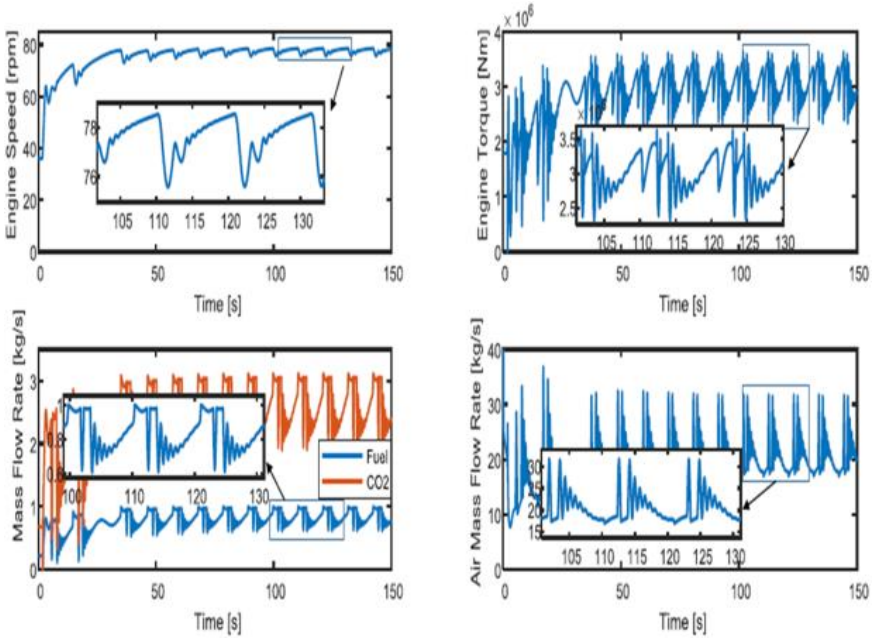

Figure 5. Predicted system response at λ/L_{PP}=1

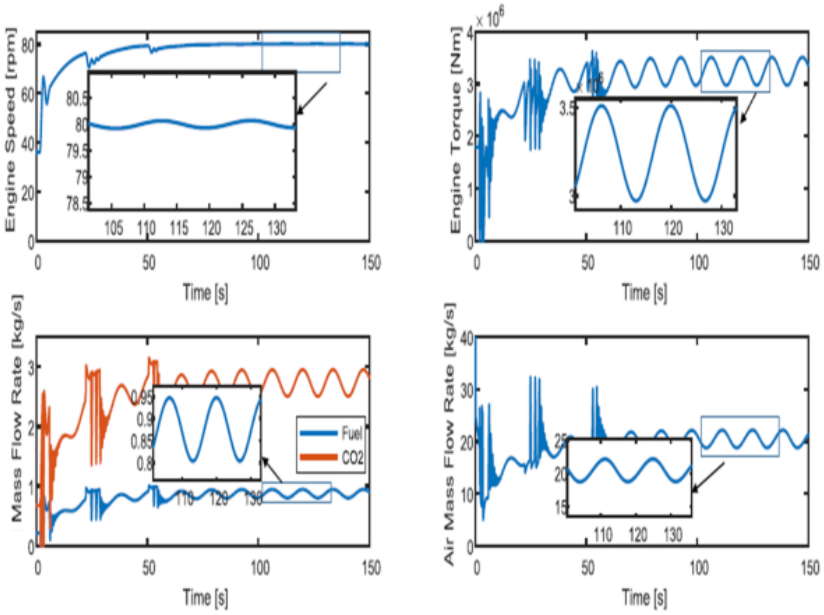

Figure 6. Predicted system response at λ/L_{PP}=1.5

and CO_2 emission are in the range of 0.57 to 0.98 kg/s and 1.77 to 3.05 kg/s, respectively, which is accompanied by 7 oscillation points. Air consumption is between 16.6 to 33.4 kg/s with 6 oscillation points. As shown in Figure 8, the amplitude of engine power fluctuations in the steady state is from 17.6 to 29.1 MW. In addition, the number of oscillation points is 7.

At λ/L_{PP} of 1, as can be seen in Figure 5, the amplitude of the engine speed fluctuations in the steady state is from 75.6 to 78.5 rpm. The number of oscillating points is 8. Torque oscillations range is of

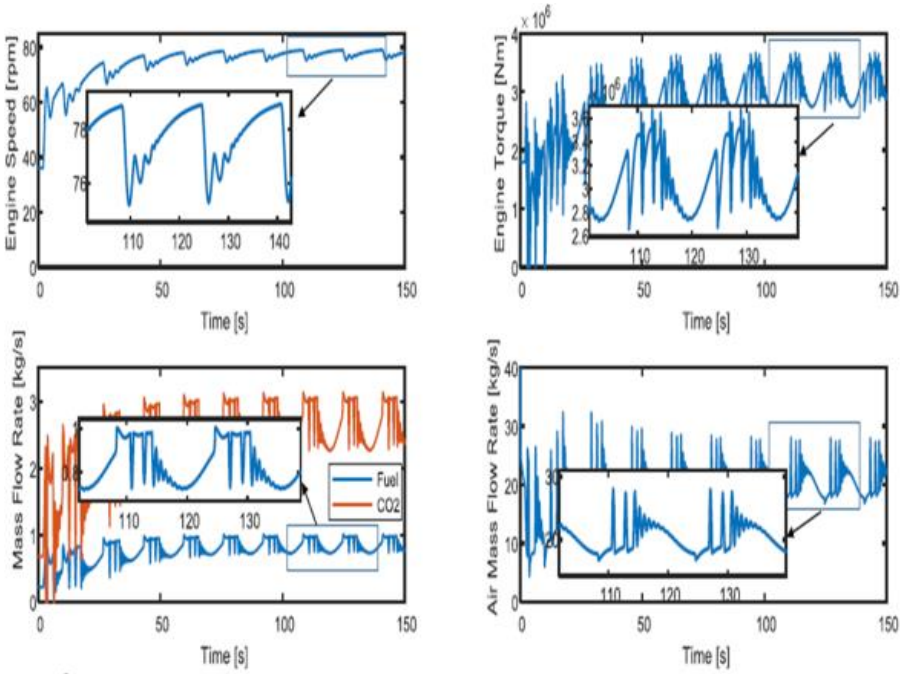

Figure 7. Predicted system responses at $\lambda/L_{PP}=2$

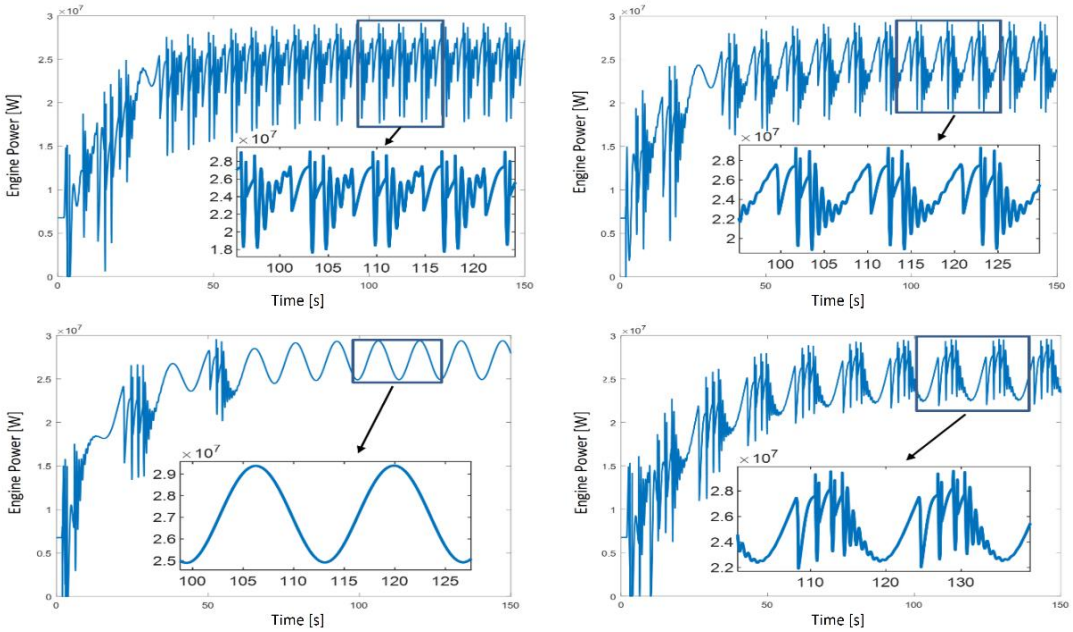

Figure 8. Predicted engine power at: (a) $\lambda/L_{PP}=0.5$; (b)$\lambda/L_{PP}=1$; (c) $\lambda/L_{PP}=1.5$; (d) $\lambda/L_{PP}=2$

2.3 to 3.6 MNm with 13 oscillation points. Fuel consumption and CO_2 emission are in the range of 0.60 to 0.99 kg/s and 1.86 to 3.08 kg/s, respectively, with 12 oscillation points. Air consumption is between 16.9 to 31.7 kg/s with 11 oscillation points. As can be seen in Figure 8, the range of power fluctuations in the steady state is from 18.8 to 29.2 MW. The number of oscillation points is 11.

At λ/L_{PP} of 1.5, as shown in Figure 6, the range of engine speed fluctuations is changed from 79.9 to 80 rpm. As can be seen the number of oscillation points is 2. Torque fluctuations range is 2.97 to 3.51 MNm with 2 oscillation points. Fuel consumption and CO_2 emission are in the range of 0.80 to 0.94 kg/s and 2.49 to 2.92 kg/s, respectively, which are accompanied by 2 oscillation points. Air consumption is between 18.75 to 22.17 kg/s with 2 oscillating points. As shown in Figure 8, the range of power fluctuations in the steady state is from 24.9 to 29.3 MW with number of 2 oscillation points.

At λ/L_{PP} of 2, as can be seen in Figure 7, the amplitude of the engine speed fluctuations in the steady state is 75.18 to 78.92 rpm. The number of oscillation points is 8. Torque fluctuations interval is from 2.66 to 3.67 MNm with 15 oscillation points. Fuel consumption and CO_2 emission are in the range of 0.72 to 1 kg/s and 2.24 to 3.114 kg/s, respectively, which are accompanied by 14 oscillation points. Air consumption is from 16.7 to 28.1 kg/s with 11 oscillation points. As can be seen in Figure 8, the interval of engine power fluctuations in the steady state is from 21.9 to 29.5 MW. The number of oscillation points is 14.

As shown in these figures, when fuel consumption increases, the air flow does not increase simultaneously, and the air consumption diagram shows a delay, which is due to the inertia of the turbocharger system and its response. When the propeller coming out of the water, an increase in propeller speed occurs and as a result the torque will decrease and the power has a decreasing trend. As soon as the ship's propeller is completely submerged in the water, the torque increases and the speed decreases. As a result, the decreasing trend of power becomes an increasing trend. The results related to changes in engine performance parameters and the number of oscillation points can be seen in Table 3. As can be seen, there is the highest number of oscillation points and on the other hand the highest changes in engine speed at λ/L_{PP} of 2. At λ/L_{PP} of 0.5, the largest changes in torque, fuel consumption, CO_2 emission and air consumption are observed. On the other hand, the smallest changes in engine speed, torque, fuel consumption, CO_2 emission and air consumption can be seen at λ/L_{PP} of 1.5. By comparing the results, it can be seen that as the λ/L_{PP} ratio increases, the period of oscillations and the number of fluctuations in each period will also increase. At λ/L_{PP} of 1.5, as can be seen from the responses, the graph is smooth and no fluctuations are seen in this case.

TABLE 3. Changes in engine performance parameters

λ/LPP	**0.5**	**1**	**1.5**	**2**
Speed changes (rpm)/ number of oscillation points	3/ 6	2.9/ 8	0.1/ 2	3.74/ 8
Torque changes (MNm)/ number of oscillation points	1.4/9	1.3/13	0.54/ 2	1.01/ 15
Fuel consumption changes (kg/s)/ number of oscillation points	0.41/7	0.39/12	0.14/ 2	0.28/ 14
CO_2 changes (kg/s)/ number of oscillation points	1.28/7	1.22/12	0.43/ 2	0.874/14
Air consumption changes (kg/s)/ number of oscillation points	16.8/6	14.8/11	3.42/ 2	11.4/ 11
Power changes (MW)/ number of oscillation points	11.5/7	10.4/11	4.4 / 2	7.6/ 14

5.CONCLUSION

A very large crude oil carrier ship is successfully modeled and through implementation of Simulink environment, the behavior of the engine such as power, fuel consumption and the amount of emissions in dealing with waves at different wavelengths have been investigated. The validity and accuracy of the model were examined through the voyage report of a VLCC available. The accuracy of the model results with good compliance with the VLCC report shows that the model is reliable. In the modeling process, the various components of the ship, including the hull and forces on it, the engine and its components, the power transmission shafts and the propeller were considered. The study shows that the effect of waves with different wavelength on engine behavior cannot be ignored. The effect of changing the wavelength can be seen as fluctuations in the behavior of the engine, which can cause problems in the ship's powertrain system if repeated. The results of the effect of λ/L_{PP} of 0.5, 1, 1.5 and 2 in violent stormy sea conditions on the engine show, with the exception of λ/L_{PP} of 1.5, in other cases with increasing λ/L_{PP}, the number of oscillating points in

the behavior of the engine performance parameters increases. The least changes in engine performance parameters are seen at λ/L_{pp} of 1.5, while with the exception of λ/L_{pp} of 2, where the speed variations are higher than other λ/L_{pp} values, the trend of changes in other engine performance parameters is decreasing with increasing λ/L_{pp} values. As a result, the effects of waves with different wavelengths should not be neglected in the design phase of the ship's propulsion system.

6. REFERENCES

1. Molina, S., Guardiola, C., Martín, J. and García-Sarmiento, D., "Development of a control-oriented model to optimise fuel consumption and nox emissions in a di diesel engine", ***Applied Energy***, Vol. 119, (2014), 405-416, https://doi.org/10.1016/j.apenergy.2014.01.021
2. Liu, J., Yang, F., Wang, H., Ouyang, M. and Hao, S., "Effects of pilot fuel quantity on the emissions characteristics of a cng/diesel dual fuel engine with optimized pilot injection timing", ***Applied Energy***, Vol. 110, (2013), 201-206, https://doi.org/10.1016/j.apenergy.2013.03.024
3. Rutherford, D. and Comer, B., "The international maritime organization's initial greenhouse gas strategy", (2018).
4. Diesel, M. and Turbo, S., "Basic principles of ship propulsion", ***MAN Diesel & Turbo Publication***, (2004).
5. Naghipour, M., "Estimation of hydrodynamic force on rough circular cylinders in random waves and currents (research note)", ***International Journal of Engineering***, Vol. 14, No. 1, (2001), 25-34.
6. Mirbagheri, S., RAJAEI, T. and MIRZAEI, F., "Solution of wave equations near seawalls by finite element method", ***International Journal of Engineering, Transactions A: Basics***, Vol. 21, No. 1, (2008), 1-16.
7. Farhadi, A., "Investigating the third order solitary wave generation accuracy using incompressible smoothed particle hydrodynamics", ***International Journal of Engineering, Transactions C: Aspects***, Vol. 29, No. 3, (2016), 426-435, doi: 10.5829/idosi.ije.2016.29.03c.17.
8. Bayani, R., Farhadi, M., Shafaghat, R. and Alamian, R., "Experimental evaluation of irwec1, a novel offshore wave energy converter", ***International Journal of Engineering***, Vol. 29, No. 9, (2016), 1292-1299, doi: 10.5829/idosi.ije.2016.29.09c.15.
9. Yazdi, H., Shafaghat, R. and Alamian, R., "Experimental assessment of a fixed on-shore oscillating water column device: Case study on oman sea", ***International Journal of Engineering, Transactions C: Aspects***, Vol. 33, No. 3, (2020), 494-504, doi: 10.5829/ije.2020.33.03c.14.
10. Taskar, B. and Steen, S., "Analysis of propulsion performance of kvlcc2 in waves", in Proceedings of the Fourth International Symposium on Marine Propulsors (Volume I), International Symposiums on Marine Propulsors Texas. (2015).
11. Taskar, B., Yum, K.K., Steen, S. and Pedersen, E., "The effect of waves on engine-propeller dynamics and propulsion performance of ships", ***Ocean Engineering***, Vol. 122, (2016), 262-277, https://doi.org/10.1016/j.oceaneng.2016.06.034
12. Kyrtatos, N., Theodossopoulos, P., Theotokatos, G. and Xiros, N., "Simulation of the overall ship propulsion plant for performance prediction and control", ***Transactions-Institute of Marine Engineers Series C***, Vol. 111, (1999), 103-114, doi.
13. Kayano, J., Yabuki, N., Sasaki, N. and Hiwatashi, R., "A study on the propulsion performance in the actual sea by means of full-scale experiments", ***TransNav: International Journal on Marine Navigation and Safety of Sea Transportation***, Vol. 7, No. 4, (2013), 521-526, https://doi.org/10.12716/1001.07.04.07
14. Larroudé, V., Chenouard, R., Yvars, P.-A. and Millet, D., "Constraint based approach for the steady-state simulation of complex systems: Application to ship control", ***Engineering Applications of Artificial Intelligence***, Vol. 26, No. 1, (2013), 499-514, https://doi.org/10.1016/j.engappai.2012.07.003
15. Scappin, F., Stefansson, S.H., Haglind, F., Andreasen, A. and Larsen, U., "Validation of a zero-dimensional model for prediction of nox and engine performance for electronically controlled marine two-stroke diesel engines", ***Applied Thermal Engineering***, Vol. 37, (2012), 344-352, doi. https://doi.org/10.1016/j.applthermaleng.2011.11.047
16. Bazari, Z., "Diesel exhaust emissions prediction under transient operating conditions", ***SAE Transactions***, (1994), 1004-1019, https://doi.org/10.4271/940666
17. Hendricks, E., "Mean value modelling of large turbocharged two-stroke diesel engines", ***SAE Transactions***, (1989), 986-998, https://doi.org/10.4271/890564
18. Yum, K.K., Taskar, B., Pedersen, E. and Steen, S., "Simulation of a two-stroke diesel engine for propulsion in waves", ***International Journal of Naval Architecture and Ocean Engineering***, Vol. 9, No. 4, (2017), 351-372, doi. https://doi.org/10.1016/j.ijnaoe.2016.08.004
19. Theotokatos, G. and Tzelepis, V., "A computational study on the performance and emission parameters mapping of a ship propulsion system", ***Proceedings of the Institution of Mechanical Engineers, Part M: Journal of Engineering for the Maritime Environment***, Vol. 229, No. 1, (2015), 58-76, https://doi.org/10.1177/1475090213498715
20. Xiros, N., "Robust control of diesel ship propulsion, Springer Science & Business Media, (2012).
21. Heywood, J.B., "Internal combustion engine fundamentals, McGraw-Hill Education, (2018).
22. IMO, T.I., "Greenhouse gas study", Executive Summary and Final Report, London, (2014).
23. Minsaas, K., Faltinsen, O. and Persson, B., "On the importance of added resistance, propeller immersion and propeller ventilation for large ships in a seaway", (1983).
24. Faltinsen, O.M., "Prediction of resistance and propulsion of a ship in a seaway", in Proceedings of the 13th symposium on naval hydrodynamics, Tokyo, 1980. (1980).
25. Ueno, M., Tsukada, Y. and Tanizawa, K., "Estimation and prediction of effective inflow velocity to propeller in waves", ***Journal of Marine Science and Technology***, Vol. 18, No. 3, (2013), 339-348, https://doi.org/10.1007/s00773-013-0211-8
26. Gholami, A., Jazayeri, S.A. and Esmaili, Q., "Marine powertrain simulation for design and operational performance evaluation", ***International Journal of***

Powertrains, Vol. 9, No. 4, (2020), 289-314, doi: 10.1504/IJPT.2020.111232.

27. Holtrop, J. and Mennen, G., "An approximate power prediction method", ***International Shipbuilding Progress***, Vol. 29, No. 335, (1982), 166-170.
28. Liu, S., Shang, B. and Papanikolaou, A., "On the resistance and speed loss of full type ships in a seaway", ***Ship Technology Research***, Vol. 66, No. 3, (2019), 161-179, https://doi.org/10.1080/09377255.2019.1613294
29. Safaei, A.A., Ghassemi, H. and Ghiasi, M., "Correcting and enriching vessel's noon report data using statistical and data mining methods", ***European Transport***, Vol. 67, (2018).
30. Yasukawa, H., Zaky, M., Yonemasu, I. and Miyake, R., "Effect of engine output on maneuverability of a vlcc in still water and adverse weather conditions", ***Journal of Marine Science and Technology***, Vol. 22, No. 3, (2017), 574-586, doi: 10.1007/s00773-017-0435-0.

Persian Abstract

چکیده

دراین تحقیق، به بررسی تاثیرطول موج های مختلف موج دریا بر رفتار موتور کشتی پرداخته شده است. برای این منظور یک مدل از سیستم کشتی با استفاده از روابط حاکم بر بخشهای مختلف کشتی اعم از بدنه، موتور، شفت های انتقال قدرت از موتور به پروانه و پروانه کشتی در محیط نرم افزار Matlab/Simulink پیاده سازی گردیده است. دراین تحقیق، ارتعاشات پیچشی شفت های انتقال قدرت درمدل لحاظ شده تا بتوان تحلیل دقیقتری از رفتار موتور به عنوان المان تولید قدرت سیستم پیشرانش کشتی ارائه کرد. نتایج نشان می دهد تغییرطول موج می تواند برعملکرد دینامیکی موتور تاثیر چشمگیرداشته باشد. دراین تحقیق، تأثیر نسبت های مختلف طول موج به طول کشتی (λ/L_{PP}) برابر ۰.۵ ، ۱ ، ۱.۵ و ۲ درشرایط طوفانی دریا با ارتفاع موج ۱۱.۵ مترو سرعت باد ۲۸.۵ متر بر ثانیه بررسی شده است. نتایج نشان می دهد به استثنایλ/L_{PP}برابر ۱.۵ ،درنسبتهای دیگرλ/L_{PP} تغییرات درپارامترهای عملکرد موتور مانند گشتاور، مصرف سوخت و هوا، میزان انتشار CO_2 و توان باافزایش طول موج، کاهش می یابد. بیشترین تغییرات در سرعت موتور مربوط به λ/L_{PP}برابر ۲ است. نتایج نشان می دهد با کاهش طول موج، دوره نوسانات کاهش می یابد. با افزایش نسبت طول موج به طول کشتی، تعداد نقاط نوسانی در رفتار موتور افزایش می یابد و کمترین تعداد نقاط نوسانی را میتوان در λ/L_{PP} برابر ۱.۵ مشاهده نمود. این مطالعه اهمیت تاثیرات طول موج دریا به عنوان یکی از مهمترین پارامترهای فیزیکی دریا را برجسته می کند که نباید در مرحله طراحی سیستم پیشرانه کشتی و انتخاب موتور نادیده گرفته شود.